Neuron, Vol. 43, 81–94, July 8, 2004, Copyright ©2004 by Cell Press

Arp2/3 Is a Negative Regulator of Growth Cone Translocation

Geraldine A. Strasser,[1] Nazimah Abdul Rahim,[2] Kristyn E. VanderWaal,[2] Frank B. Gertler,[1] and Lorene M. Lanier[2,*]

[1]Biology Department
Massachusetts Institute of Technology
Cambridge, Massachusetts 02139

[2]Department of Neuroscience
University of Minnesota
Minneapolis, Minnesota 55455

Summary

Arp2/3 is an actin binding complex that is enriched in the peripheral lamellipodia of fibroblasts, where it forms a network of short, branched actin filaments, generating the protrusive force that extends lamellipodia and drives fibroblast motility. Although it has been assumed that Arp2/3 would play a similar role in growth cones, our studies indicate that Arp2/3 is enriched in the central, not the peripheral, region of growth cones and that the growth cone periphery contains few branched actin filaments. Arp2/3 inhibition in fibroblasts severely disrupts actin organization and membrane protrusion. In contrast, Arp2/3 inhibition in growth cones minimally affects actin organization and does not inhibit lamellipodia protrusion or de novo filopodia formation. Surprisingly, Arp2/3 inhibition significantly enhances axon elongation and causes defects in growth cone guidance. These results indicate that Arp2/3 is a negative regulator of growth cone translocation.

Introduction

During development of the nervous system, axons and dendrites extend over significant distances to form synaptic connections. To make these connections accurately, growth cones must detect a vast array of diffusible and surface bound guidance molecules present in the extracellular environment (Tessier-Lavigne and Goodman, 1996; Yu and Bargmann, 2001). Binding of these guidance cues to receptors on the growth cone surface activates intracellular signaling cascades whose downstream targets include proteins that regulate the growth cone cytoskeleton (Dickson, 2002; Koleske, 2003; Luo, 2002). Modification of the cytoskeleton results in selective protrusion and retraction of the growth cone, driving growth cone motility and guiding axons and dendrites to their appropriate synaptic targets.

The growth cone has been operationally divided into three main compartments: the distal peripheral region, the transition region, and the proximal central region. The peripheral region is an actin-rich region containing abundant filopodia that play a crucial role in pathfinding (Bentley and Toroian-Raymond, 1986; Chien et al., 1993; Gomez and Letourneau, 1994; Kim et al., 2002; Kuhn et al., 1998; Zheng et al., 1996). These filopodia are dynamic structures comprised of long, bundled actin filaments. Between the filopodia lie thin regions known as lamellipodial veils. The transition region contains a dense network of actin filaments, actin arcs, and motile actin structures known as intrapodia (Dent and Kalil, 2001; Rochlin et al., 1999; Schaefer et al., 2002). The central region contains a relatively sparse network of actin filaments and abundant microtubules. These microtubules are often bundled or looped, but they also stochastically explore the peripheral region, where they contribute to pathfinding (Buck and Zheng, 2002; Dent and Kalil, 2001; Lin and Forscher, 1993; Tanaka et al., 1995; Zhou et al., 2002). Directed growth cone motility in response to extracellular cues is produced by the coordinated regulation of actin and microtubule networks (Dent and Kalil, 2001; Suter et al., 1998; Zhou et al., 2002).

Studies in motile cells such as fibroblasts have identified a large variety of factors that are involved in the organization and modification of the actin cytoskeleton (Pollard and Borisy, 2003), and in some cases these proteins have been shown to be functionally important in growth cones (Dickson, 2002). Actin binding proteins are classified according to their activities. Capping proteins like CapZ and anticapping proteins like the Ena/VASP proteins bind the polymerizing ends of actin filaments and regulate filament length (Bear et al., 2002; Caldwell et al., 1989; Cooper and Schafer, 2000; Lanier et al., 1999; Wills et al., 1999). Bundling and crosslinking proteins like fascin and filamin bind to preformed filaments and regulate their organization and stability (Cohan et al., 2001; Kureishy et al., 2002; Stossel et al., 2001). Severing proteins like gelsolin and ADF/cofilin bind actin filaments and cause them to depolymerize (Cooper and Schafer, 2000; Gungabissoon and Bamburg, 2003; Lu et al., 1997). Membrane linking proteins like those of the Ezrin/Radixin/Moesin family (ERMs) link actin filaments to the plasma membrane (Bretscher et al., 2002; Paglini et al., 1998). Finally, nucleating proteins like formins and Arp2/3 induce the formation of new actin filaments (Kobielak et al., 2004; Pollard, 2002; Pollard and Beltzner, 2002). Differential activation of these actin binding proteins by multiple signaling pathways is key to cell motility.

Arp2/3 is one of the most extensively studied actin binding proteins (Weaver et al., 2003). The Arp2/3 complex is composed of seven evolutionarily conserved proteins, known as Arp2, Arp3, p41-Arc, p34-Arc, p21-Arc, p20-Arc, and p16-Arc in mammals (Machesky et al., 1997; Welch et al., 1997a). Arp2/3 has been shown to nucleate the polymerization of actin monomers in vitro by binding to pre-existing actin filaments and inducing the formation of a new filament as a branch (Amann and Pollard, 2001). Ultrastructural studies of fibroblast lamellipodia show that Arp2/3 is found at characteristic Y-shaped 70° branches in the actin cytoskeleton (Svitkina and Borisy, 1999). In vivo, Arp2/3 induces the formation of a network of short, branched filaments, called a "dendritic array." Polymerizing dendritic arrays can

*Correspondence: lanie002@umn.edu

generate the protrusive force that drives many types of actin-based motility. For example, formation of a dendritic array is essential for generating the actin-based "comet tails" that propel intracellular bacteria such as *Listeria monocytogenes* through the cytoplasm of infected cells (May et al., 1999; Welch et al., 1997b). In fibroblasts, keratocytes, and a variety of other cell types, Arp2/3 is enriched in the leading edge, where rapid actin filament polymerization generates the protrusive force that drives lamellipodia extension and forward motility (Machesky et al., 1997; Welch et al., 1997a). Inhibition of Arp2/3 by microinjection of a function-blocking antibody blocks membrane protrusion, indicating that Arp2/3 is essential for lamellipodia protrusion in fibroblasts (Bailly et al., 2001).

The Arp2/3 complex has a low level of constitutive activity and must undergo a conformational change in order to become fully activated. This conformational change can be mediated by binding to the C-terminal domain of members of the WASP/WAVE family of proteins in vitro and in vivo (Miki et al., 1996; Symons et al., 1996; Weaver et al., 2001, 2003; Weed et al., 2000). This C-terminal domain contains three regions: the verpolin-homology (V) actin binding region (Miki and Takenawa, 1998); the cofilin-homology or central (C) region; and the acidic (A) Arp2/3 binding region (Marchand et al., 2001). Constructs containing only the VCA regions are potent stimulators of Arp2/3-mediated actin polymerization in vitro but fail to localize and therefore inhibit Arp2/3 function in vivo (Machesky et al., 1999; Rohatgi et al., 1999; Winter et al., 1999). A peptide containing only the CA domains has been shown to bind to Arp2/3 with an affinity similar to VCA but fails to activate Arp2/3 activity in vitro (Hufner et al., 2001; Rohatgi et al., 1999). The CA peptide blocks activation of the Arp2/3 complex by VCA or full-length WASP/Scar proteins in vitro and has been used in vivo to inhibit Arp2/3 activity (Falet et al., 2002; Hufner et al., 2002).

Arp2/3 is regarded as a key player in most models of actin-based motility. Although Arp2/3 has been shown to be essential for embryonic CNS axon morphology in *Drosophila* (Zallen et al., 2002), the role of Arp2/3 actin nucleating activity in the formation and motility of the growth cone has not been studied. It has been assumed that the primary role of Arp2/3 in growth cones would be to generate a dendritic actin array that drives lamellipodial veil protrusion. Growth cones are, however, dominated by filopodia containing unbranched actin filaments, and the Arp2/3 complex is generally absent from filopodia (Svitkina and Borisy, 1999). Recently, Svitkina and colleagues proposed a "convergent elongation model" of filopodia formation that suggests a role for Arp2/3 in filopodia formation. In this model, filopodia are derived from rearrangement of elongating actin filaments into bundles (Svitkina et al., 2003; Vignjevic et al., 2003). The role of Arp2/3 is limited to the initial nucleation of filaments into a dendritic array; a subset of these filaments then elongate and are subsequently bundled together by fascin to form a filopodium.

Given its key role in other types of actin-based motility, we sought to determine if Arp2/3 plays a similar role in growth cone morphology and motility. To do this, we used the N-WASP CA or Wave-1 VCA peptides to block Arp2/3 activity in cultured primary neurons. Surprisingly, inhibition of Arp2/3 in neurons had little affect on growth cone morphology or filopodia formation and appeared to enhance axon elongation. In fibroblasts, inhibition of Arp2/3 severely disrupted the lamellipodial actin cytoskeleton, inhibited actin tail formation by *Listeria monocytogenes*, and altered lamellipodial protrusion. Our findings suggest that in the growth cone, Arp2/3 is a negative regulator of neurite outgrowth and may be important for the pathfinding role of the cytoskeleton.

Results

Arp2/3 Is Enriched in the Central Region of the Growth Cone

Although Arp2/3 is a key player in many types of actin-based motility, its role in the formation and motility of the growth cone remains unclear. Both the dendritic array model of lamellipodia protrusion and the convergent extension model of filopodia formation require Arp2/3 to be enriched at the periphery of the fibroblast. If either model is directly applicable to growth cone motility, Arp2/3 should be enriched in an analogous region in the growth cone. Surprisingly, immunofluorescence localization revealed that Arp2/3 is enriched in the neurite shaft and central region of the growth cone but not the peripheral region of the growth cone (Figure 1). Similar results were obtained with antisera to Arp3, p34-Arc, and p21-Arc (Figures 1A–1C) in growth cones from hippocampal neurons (Figure 1) and dorsal root ganglia (DRG) neurons (data not shown). Staining of Rat2 fibroblasts with the same antibodies under identical fixation conditions confirmed that, as expected, Arp2/3 is enriched in the fibroblast periphery/lamellipodia (Figures 1H–1J).

To verify the immunostaining results, Arp2/3 was localized using a p21-EGFP fusion protein. As with the antisera staining, p21-EGFP was highly enriched in the fibroblast periphery (Figure 1K) but was restricted to the neurite shaft and central region of the growth cone (Figures 1D–1G). Similar Arp2/3 localization was seen in small (Figures 1A and 1D) and large (Figures 1B and 1F) growth cones, in terminal (Figures 1A, 1B, and 1D) and collateral (Figures 1F and 1G) branch growth cones, and in dendrite growth cones (Figure 1E). Since small dynamic growth cones are likely to be translocating, while large growth cones are likely to be paused (Kim et al., 1991; Mason and Erskine, 2000; Szebenyi et al., 2001; Tosney and Landmesser, 1985), this indicates that Arp2/3 localization does not change with motility. Under no circumstances was Arp2/3 enrichment detected in the growth cone periphery. Finally, Arp2/3 localization in the growth cone central region was resistant to prepermeabilization (data not shown), suggesting that Arp2/3 in the central region of the growth cone is associated with the cytoskeleton.

Actin Organization in the Growth Cone Periphery

Arp2/3 activity is essential for the formation of the highly branched dendritic array of actin filaments found at the edge of the protruding fibroblast lamellipodia. If Arp2/3 plays a similar role in the growth cone, we would expect to see similar branched actin arrays in the peripheral region of the growth cone. To analyze the supramolecu-

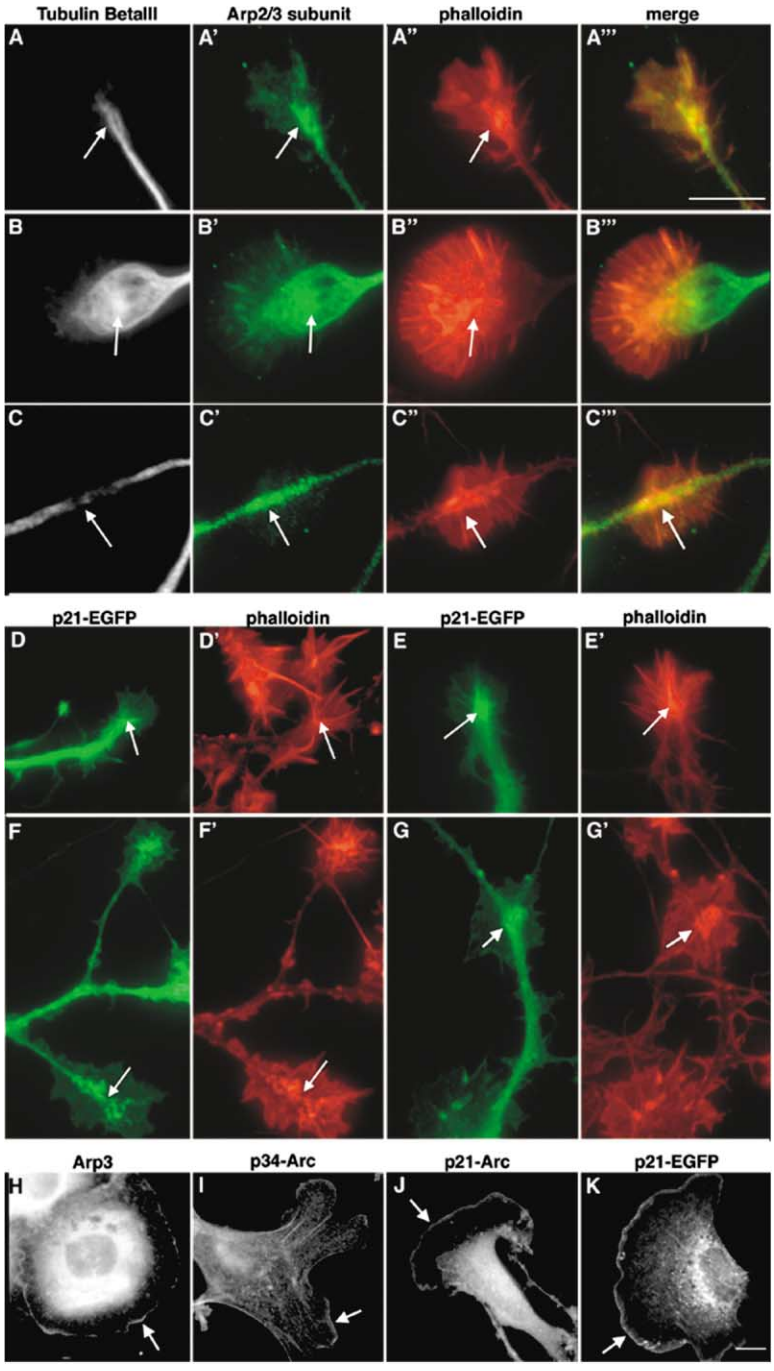

Figure 1. Arp2/3 Localization in Growth Cones

(A–C) Embryonic hippocampal neurons labeled with antibodies to Arp3 (A′), p34-Arc (B′), or p21-Arc (C′), anti-tubulin β III (A–C), and phalloidin to visualize filamentous actin (A″–C″). Arp2/3 and phalloidin staining are merged and overlap appears yellow (A‴–C‴). Arp2/3 is enriched in the central regions of small growth cones (A–A″, arrows), of large growth cones with looped microtubules (B–B″, arrows), and in filopodia-rich regions of the neurite shaft (C′, C″, arrow), where decreased tubulin staining (C, arrow) correlates with branch emergence.

(D–G) Embryonic hippocampal neurons infected with recombinant adenovirus expressing p21-EGFP (D–G) and stained with phalloidin (D′–G′). Cells were also labeled with anti-tubulin β III to identify neurons (data not shown). p21-EGFP is enriched in the central region of small axon growth cones (D, arrow), dendrite growth cones (E, arrow), large collateral branch growth cones (F), and filopodia-rich regions of the neurite shaft (G and G′, arrows).

(H–K) Control Rat2 fibroblasts labeled with antibodies to Arp3 (H), p34-Arc (I), or p21-Arc (J), and expressing p21-EGFP (K). In fibroblasts, Arp2/3 is enriched in the peripheral lamellipodia (arrows in H–K). There is also a detergent-extractable cytoplasmic pool (visible here because cells were not treated with detergent before fixation). Scale bars equal 10 μm for all growth cones (as shown in A‴) and 10 μm for all fibroblasts (as shown in K).

lar organization of the actin filaments in the growth cone, we used the platinum replica method of Svitkina et al. (1995), modified to preserve the overall growth cone morphology and visualize the actin filaments. As expected, the fibroblast periphery contains a dense dendritic array (Figures 2A–2A′).

In contrast, the actin network in the growth cone periphery appears to be dominated by thick bundles of filaments organized into filopodia, with an array of very long filaments underlying the lamellipodial veil (Figures 2B and 2C). The veil region is quite dense with long filaments, and although they frequently cross over each other, we identified very few structures resembling classic Arp2/3-generated Y branch structures (Svitkina and Borisy, 1999). As with the localization studies, similar results were obtained in both large and small growth cones (Figures 2B and 2C, respectively) and in dendrite growth cones (data not shown). Furthermore, analysis of lamellipodia veils between growth cone filopodia revealed that neither concave nor convex growth cone lamellipodia (Figures 2B′ and 2C′) contained structures resembling the Arp2/3-dependent dendritic arrays formed in fibroblasts (Figure 2A′). Together, these findings suggest that, in contrast to fibroblasts, Arp2/3 may

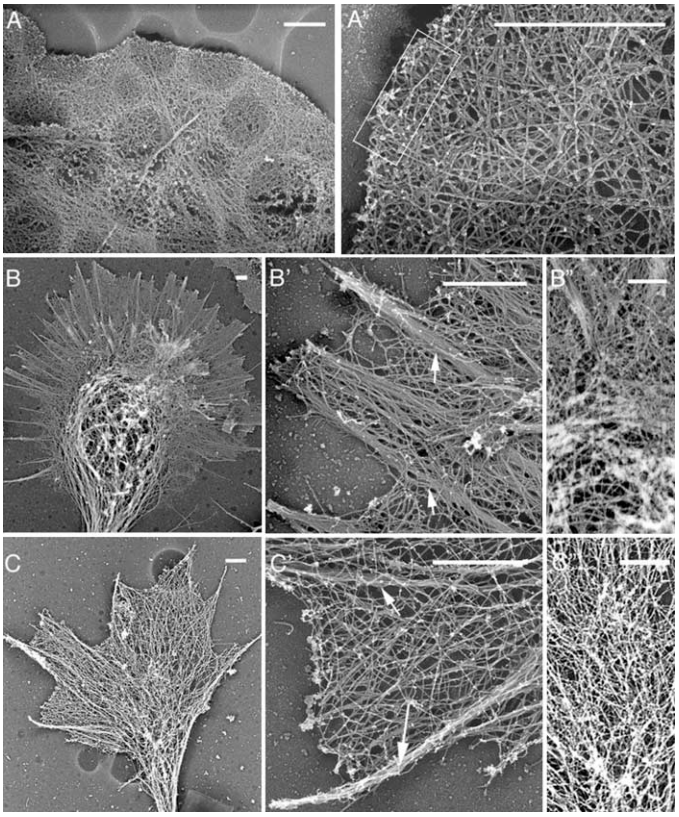

Figure 2. Comparison of Actin Filament Organization in Fibroblasts and Neuronal Growth Cones

The actin cytoskeleton is visualized in Rat2 fibroblasts (A) and growth cones from embryonic hippocampal neurons (B and C) using platinum replica electron microscopy. Lower-magnification images reveal the overall morphology and relative size (A–C). Higher-magnification images reveal details of the actin organization in the periphery (A′–C′). Individual filaments can be seen in (A′)–(C′). The dense dendritic array is visible in the boxed region of the fibroblast (A′). Prominent actin bundles are visible in the growth cone (arrows, B′ and C′). High-magnification images of the growth cone central region (B″ and C″) show the dense network of actin filaments and microtubules. Scale bars equal 1 μm.

not be a major determinant of actin organization at the growth cone periphery.

Inhibition of Arp2/3 Dramatically Alters Fibroblast Actin Ultrastructure and Lamellipodial Dynamics

To test the requirement for Arp2/3 in vivo, Arp2/3 activity was functionally inhibited by expressing amino acids 468–505 of the N-WASP CA domains fused to enhanced green fluorescent protein (EGFP-CA). Residues 468–505 of the bovine N-WASP include the entire sequence required for full-strength binding to Arp2/3 (Zalevsky et al., 2001) and the "KRSK" sequence that was originally described as the "cofilin homology" domain and which was shown to play a role in neurite extension in PC12 cells (Banzai et al., 2000). Constructs containing this sequence bind to, but do not activate, Arp2/3 and do not bind to actin (Hufner et al., 2001; Rohatgi et al., 1999). Similar constructs have been shown to inhibit the actin-based motility of *Listeria monocytogenes* (May et al., 1999).

As predicted, the EGFP-CA construct displaced Arp2/3 from the fibroblast lamellipodia and altered the actin structures (Figures 3A and 3B). The displaced Arp2/3 was sensitive to detergent extraction (see Supplemental Figure S1 at http://www.neuron.org/cgi/content/full/43/1/81/DC1), indicating that it is no longer associated with the cytoskeleton. The in vivo efficacy of EGFP-CA was further demonstrated by its ability to inhibit *Listeria* motility in fibroblasts (Figure 3D). Control cells expressing EGFP appeared normal and supported *Listeria* motility (Figure 3C). Closer examination of cells expressing EGFP-CA by EM revealed an acute disruption of the dendritic array (Figures 4A–4D). Actin filaments were still present but were often extremely long, unbranched, and oriented parallel to the cell membrane (Figure 4C) or organized into bundles (Figure 4D). By contrast, a normal dendritic array morphology could been seen in the lamellipodia of uninfected cells (Figure 4A) and cells expressing EGFP alone (Figure 4B). Finally, as previously shown using Arp2/3 function blocking antibodies (Bailly et al., 2001), expression of EGFP-CA altered membrane protrusion and lamellipodia formation (Figures 4E and 4F).

Inhibition of Arp2/3 Minimally Affects Growth Cone Actin Organization and Dynamics

To determine the effect of Arp2/3 inhibition on growth cone dynamics and translocation, we used cultured primary embryonic hippocampal neurons, which form a single axon and multiple dendrites in vitro, just as they do in vivo (Goslin and Banker, 1998). Because it is difficult to obtain high-transfection efficiency in neurons using standard techniques, replication-defective recombinant adenoviruses were used to express proteins in fibroblasts and neurons. As previously demonstrated for other adenoviral vectors (Le Gal La Salle et al., 1993; Meberg and Bamburg, 2000), our replication-defective adenoviruses gave consistent, high level expression with low cytotoxicity in neurons. For these and subsequent studies, infection was monitored by EGFP expression and only neurons expressing moderate levels of EGFP were analyzed.

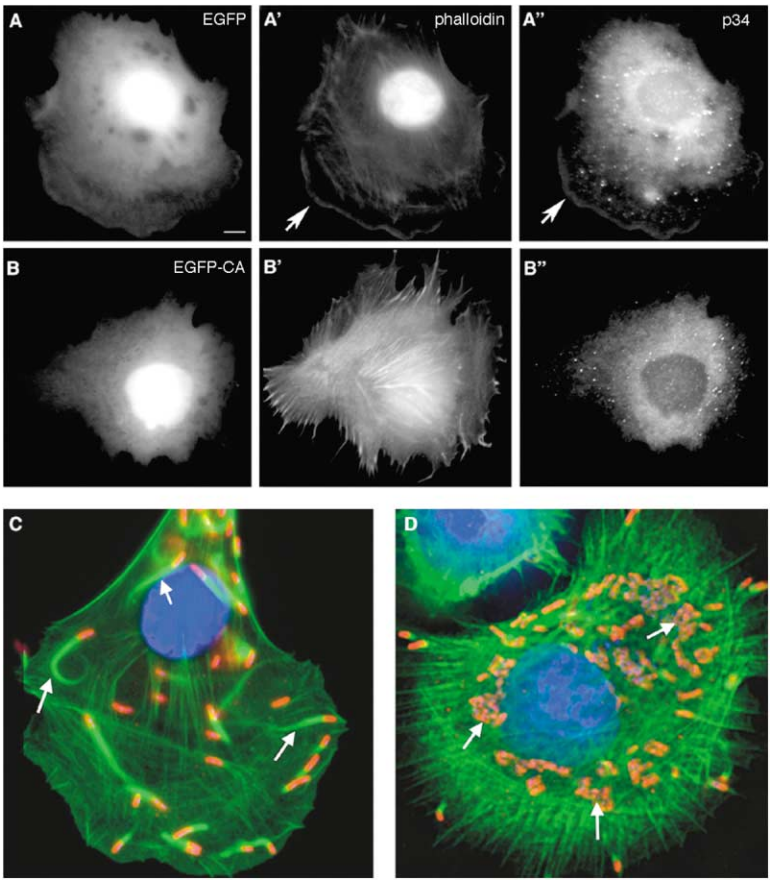

Figure 3. Controls for EGFP-CA Efficacy as an Arp2/3 Inhibitor

EGFP-CA was tested for its ability to displace Arp2/3 from the cell periphery and to inhibit *Listeria* motility.

(A and B) Rat2 fibroblasts infected with a recombinant adenoviruses expressing control EGFP (A) or EGFP-CA (B) and labeled with phalloidin (A′ and B′) and antibodies to p34-Arc (A″ and B″). In control EGFP-expressing cells, p34-Arc (A″) colocalizes with actin (A′) at the leading edge (arrows). In EGFP-CA-expressing cells, actin structures are altered (B′) and p34-Arc is no longer enriched at the periphery (B″).

(C and D) 25 hr after infection with adenoviruses, Rat2 cells were infected with *Listeria monocytogenes* and labeled with antiserum to *Listeria* (red), phalloidin (green), and DAPI (blue). EGFP is not shown in these images. In the control expressing EGFP, *Listeria* generate actin comet tails (arrows) that propel them through the cytoplasm (C). Expression of EGFP-CA inhibits tail formation, so the *Listeria* divide and form microcolonies (D, arrows); a few *Listeria* "escapees" are seen at the periphery.

If Arp2/3 has a similar role in fibroblasts and growth cones, then we would expect that inhibition of Arp2/3 would cause dramatic changes in the growth cone actin cytoskeleton. Surprisingly, growth cones of neurons expressing EGFP-CA were indistinguishable from controls by immunofluorescence (Figures 5A–5F). EGFP and EGFP-CA are found in the central region of the growth cone and in the neurite shaft (data not shown), making it difficult to detect delocalization of the Arp2/3 in EGFP-CA neurons; however, the EGFP-CA was sensitive to detergent extraction, indicating that EGFP-CA and any bound Arp2/3 are no longer associated with the cytoskeleton (data not shown). At the EM level, actin organization in control EGFP (Figure 5G) and EGFP-CA-expressing (Figures 5H and 5I) growth cones was virtually indistinguishable, though filament density was sometimes reduced in EGFP-CA-expressing growth cones (Figure 5I). Populations of control and EGFP-CA-expressing neurons both contained small growth cones (Figures 5A and 5D), large growth cones (Figures 5B and 5E), and large paused growth cones with looped microtubules (Figures 5C and 5F). This is in contrast to fibroblasts expressing even moderate levels of EGFP-CA, in which dramatic changes in the cytoskeleton were visible at both the light and EM levels (Figures 4). Consistent with the apparently normal actin cytoskeleton, growth cones expressing EGFP-CA retained the ability to form protrusive filopodia and lamellipodia (Figures 5J and 5K).

Inhibition of Arp2/3 Enhances Axon Elongation

There are two main components to growth cone motility: dynamic protrusion/retraction and translocation. The dynamic protrusion and retraction of filopodia and lamellipodia veils occurs in all growth cones, including paused growth cones. Translocation (i.e., forward movement) occurs only in elongating neurites. Our previous results suggest that Arp2/3 is not essential for dynamic protrusion and retraction in growth cones.

Surprisingly, inhibition of Arp2/3 by EGFP-CA induced a significant increase in axon length (Figures 6A–6E). As an additional control for the specificity of the CA peptide, we expressed EGFP fused to a truncated peptide containing only the "C" domain of N-WASP, which does not bind to Arp2/3 (Hufner et al., 2001). As expected, expression of this construct had no effect on axon length (Figures 6B and 6E). As a positive control, the "VCA" region of Wave-1 (another Arp2/3 activator), was expressed with a nonfused EGFP under a second CMV promoter. The VCA peptide contains an actin binding "V" domain in addition to the "CA" domains and, like CA alone, binds to Arp2/3. Although VCA will activate Arp2/3 in vitro, it disrupts Arp2/3 localization and acts as a dominant inhibitor in vivo (Machesky and Insall, 1998). As in the case of EGFP-CA, VCA expression significantly increased axon length compared to controls expressing either EGFP-C or EGFP alone (Figures 6A–6E). In addition, VCA did not cause any obvious changes in growth cone actin organization, as determined by

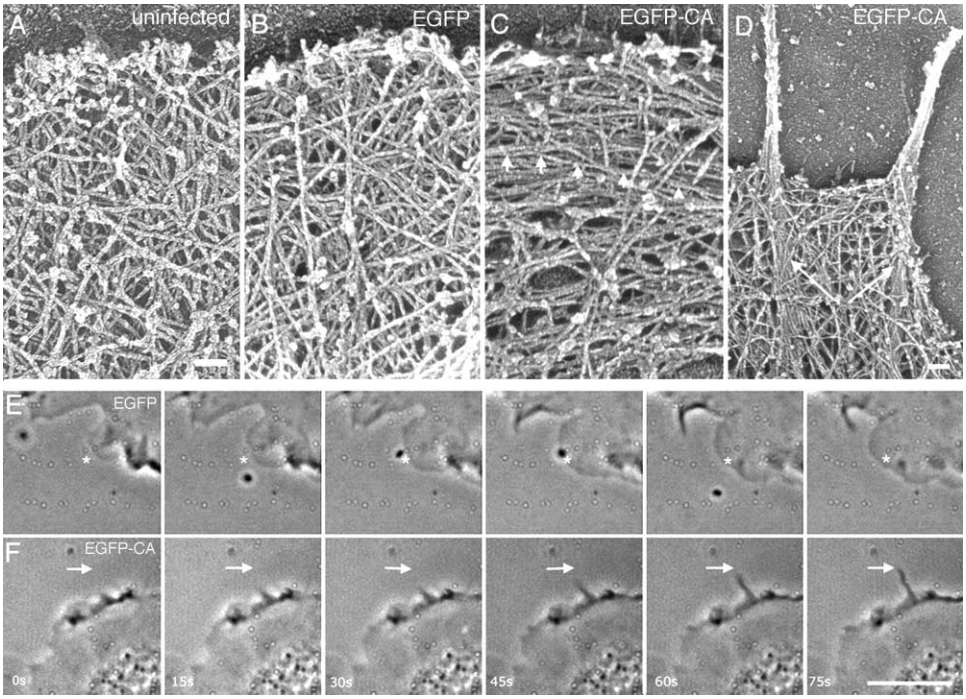

Figure 4. Inhibition of Arp2/3 Alters Fibroblast Actin Organization and Membrane Protrusion

(A–D) EM visualization of actin organization in Rat2 fibroblasts that were uninfected (A) or expressing EGFP (B) or EGFP-CA (C and D). In the controls (A and B), the periphery is dominated by short, branched filaments. In contrast, cells expressing EGFP-CA (C and D) exhibit abnormal organization, characterized by a dramatic increase in long filaments that were oriented parallel to the membrane (C, arrowheads indicate one such filament). These long filaments were occasionally bundled (D, arrows).

(E and F) Time-lapse images of Rat2 cells expressing control EGFP (E) or EGFP-CA (F) demonstrate the effect of EGFP-CA on membrane protrusion. The control (E) forms a smooth, convex protruding lamellipodium. The cell expressing EGFP-CA only forms spiky, filopodia-like structures. Star and arrow mark fixed points. Scale bars equal 0.1 μm for (A)–(D) and 10 μm for (E) and (F).

immunofluorescence (data not shown). Because axon length is directly proportional to net growth cone translocation, these results suggest that Arp2/3 may be a negative regulator of growth cone translocation.

It is interesting to note that compared to the effect on axon length, expression of EGFP-CA or VCA did not cause a significant change in dendrite length (Figure 6F). As Arp2/3 is enriched in the central region of both axonal and dendritic growth cones (Figure 1), this suggests that its activity is modulated by differential expression or activity of Arp2/3 activators. At least two Arp2/3 activators, cortactin and N-WASP, are expressed in hippocampal neurons (Figure 6G). Previous studies have shown that before neurons differentiate an axon, cortactin is enriched in the central region of all neurite growth cones (Du et al., 1998). At this stage, N-WASP is found in neurite shafts but is barely detectable in the growth cones (Figure 6H). As the neurons differentiate an axon and dendrites, N-WASP becomes preferentially enriched in the distal portion of the axon and the axon growth cone, but not in dendrite growth cones (Figures 6I and 6J).

Growth Cone Microtubules Are Affected by Arp2/3 Inhibition

We have shown that Arp2/3 appears to regulate axon elongation and is enriched in the central region of the growth cone, a region that is also rich in microtubules. Previous studies using pharmacological agents to alter actin and microtubule dynamics have shown that actin polymerization is critical for growth cone response to guidance signals, that microtubule polymerization drives axon elongation, and that coordination of actin and microtubule dynamics is critical (Bamburg et al., 1986; Bentley and Toroian-Raymond, 1986; Dent and Kalil, 2001; Marsh and Letourneau, 1984; Rochlin et al., 1999; Suter et al., 1998). To assess the effect of Arp2/3 inhibition on growth cone microtubules, we used antisera to posttranslational modifications that correlate with microtubule stability. Newly polymerized microtubules are tyrosinated, but as microtubules "age," they are detyrosinated and become acetylated (Arce et al., 1978; L'Hernault and Rosenbaum, 1985).

Although Arp2/3 inhibition did not cause an overall change in microtubule distribution in the growth cone, immunolabeling revealed that the ratio of tyrosinated to acetylated microtubules was increased when Arp2/3 was inhibited (Figures 7A–7E). The effect of EGFP-CA on microtubules was observed specifically in smaller growth cones (Figure 7E). This is consistent with the observation that Arp2/3 inhibition leads to increased axon length because translocating growth cones tend to be smaller (Kim et al., 1991; Mason and Erskine, 2000; Szebenyi et al., 2001; Tosney and Landmesser, 1985)

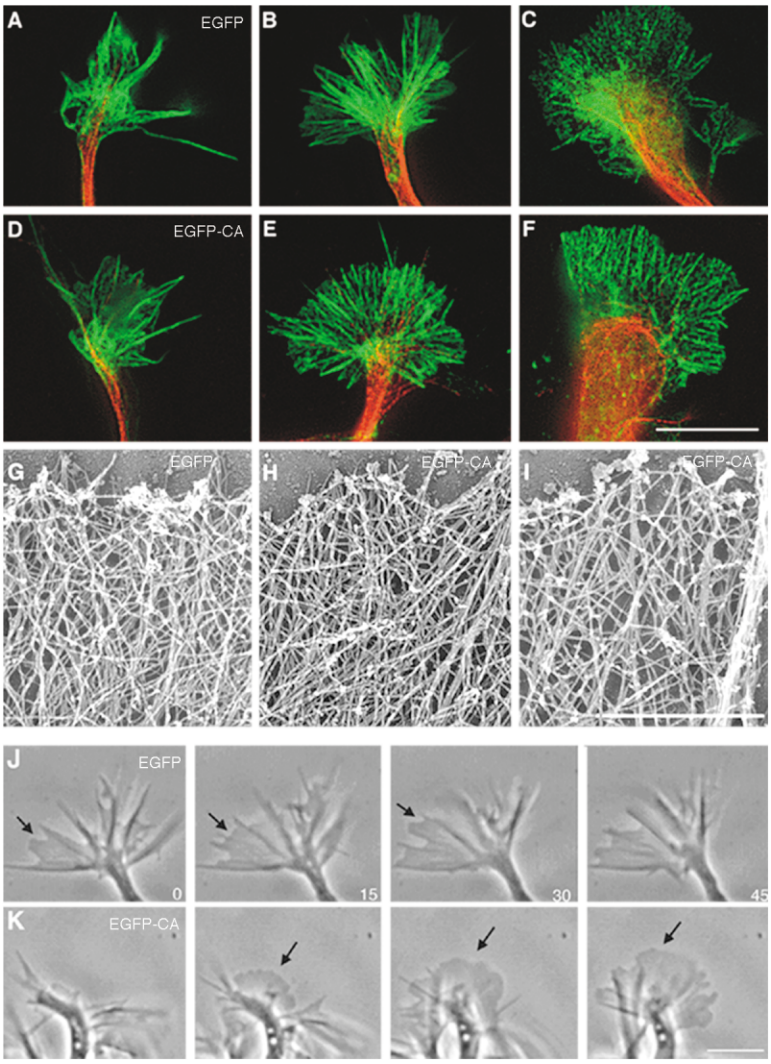

Figure 5. Arp2/3 Is not a Major Determinant of Growth Cone Actin Organization and Membrane Protrusion

(A–F) Growth cones expressing control EGFP (A–C) or EGFP-CA (D–F) were labeled with phalloidin to visualize actin (green) and with anti-tubulin β III (red). At this level, EGFP expressing growth cones are indistinguishable from those expressing EGFP-CA; both populations of growth cones contain small growth cones (A and D), large growth cones (B and E), and large paused growth cones with looped microtubules (C and F).

(G–I) At the EM level, actin organization in control EGFP (G) and EGFP-CA-expressing (H and I) growth cones is virtually indistinguishable, though filament density was sometimes reduced in EGFP-CA-expressing growth cones (I).

(J and K) Consistent with the apparently normal peripheral actin cytoskeleton, time-lapse images at 15 s intervals show that EGFP- (J) and EGFP-CA- (K) expressing growth cones are equally capable of dynamic membrane protrusion and retraction. Arrows indicate areas of protruding lamellipodia.

Scale bars equal 10 μm for (A)–(F), 1 μm for (G)–(I), and 10 μm for (J) and (K).

and enriched in tyrosinated microtubules (Bamburg et al., 1986), while stabilization of microtubules results in shorter axons (Rochlin et al., 1996).

Arp2/3 and Growth Cone Guidance

When growth cones turn to avoid an inhibitory guidance cue, filopodia collapse and dynamic microtubules are retracted from the side of the growth cone closest to the inhibitory cue (Buck and Zheng, 2002; Challacombe et al., 1997; Tanaka and Kirschner, 1995; Zhou et al., 2002). If actin is destabilized by application of low concentrations of cytochalasin B, growth cone turning is altered and dynamic microtubules fail to retract from the side of the growth cone that is in contact with the inhibitory cue (Challacombe et al., 1997). These and other studies have led to a model of growth cone turning in which actin structures direct the reorientation and stabilization of microtubules in the direction of turning.

Consistent with this model, we found that Arp2/3-dependent actin structures may play a role in growth cone turning. When neurons were plated on coverslips striped with alternating permissive and inhibitory substrates, axons of EGFP-CA-expressing neurons were more likely than controls to cross an inhibitory substrate (Figures 7F and 7G). To control for variation in the striping and in the infection rate, we compared the percent of total cells (crossing and noncrossing) that were infected and the percent of crossing cells that were infected (Figure 7H). If a treatment has no effect on the ability of neurons to cross the inhibitory stripe, then these two values should be similar. This is the case for neurons expressing EGFP alone. In contrast, if the treatment alters the ability of neurons to cross, then these values will be disproportionate. EGFP-CA-expressing neurons made up approximately 30% of crossing neurons when only about 15% of the total population was infected, suggesting that inhibition of Arp2/3 altered the ability of the growth cone to respond to the inhibitory substrate.

As discussed, the immediate response to repulsive and attractive guidance signals involves the dynamic retraction and extension of filopodia. Because Arp2/3 has been implicated in filopodia formation in other cell types (Svitkina et al., 2003), we sought to determine if

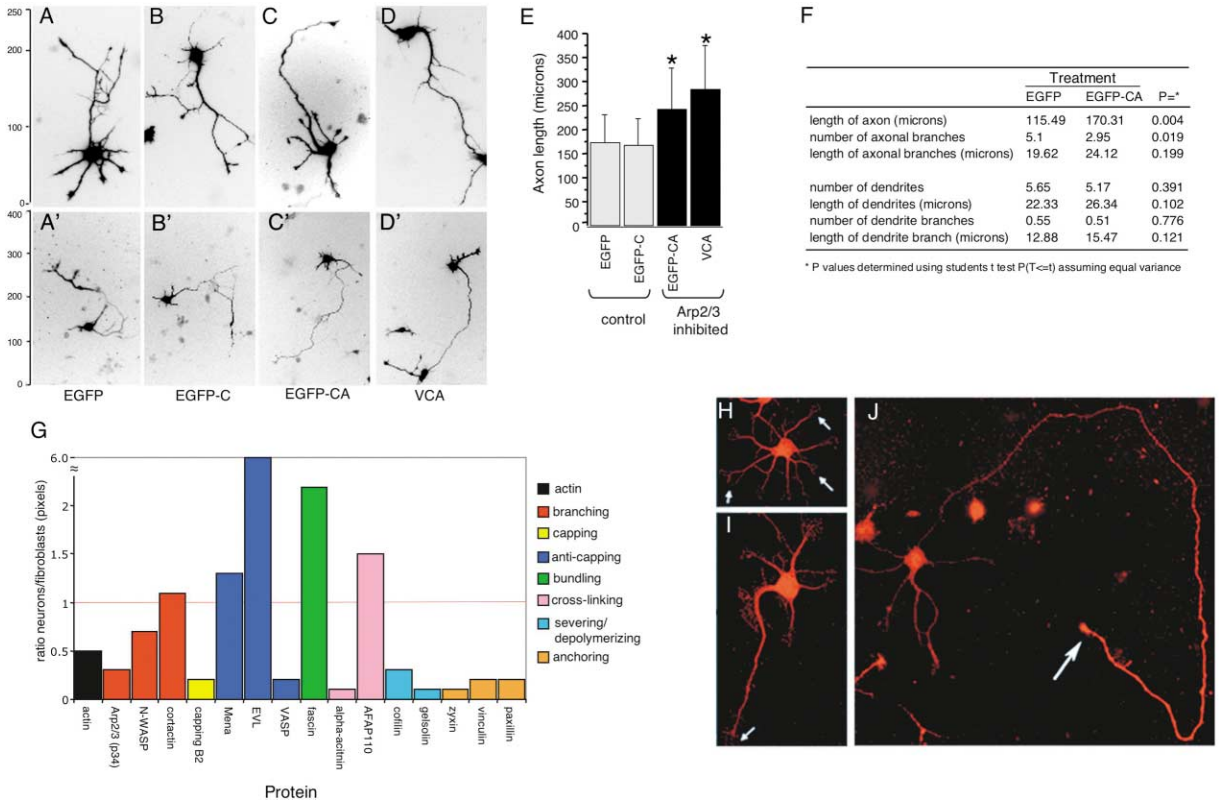

Figure 6. Inhibition of Arp2/3 Enhances Axon Elongation

(A–D) Examples of embryonic hippocampal neurons expressing EGFP (A and A′), EGFP-C (B and B′), EGFP-CA (C and C′), or VCA and EGFP (D and D′) that have axons near the mean length (A–D) or the longest length (A′–D′) for each treatment. Cultures in (A)–(E) were grown without glia conditioning and visualized by EGFP fluorescence (shown in black and white and inverted such that EGFP appears black). Staining with anti-tubulin β III was used to identify neurons (data not shown). *y* axis indicates length in microns.

(E) Analysis of the effect of EGFP, EGFP-C, EGFP-CA, and VCA on axon length. Error bars indicate ±1 standard deviation. EGFP-CA and VCA are both significantly greater than EGFP and EGFP-C ($p \leq 0.0067$), but there is no significant difference between EGFP and EGFP-C or between EGFP-CA and VCA.

(F) Breakdown of the effect of Arp2/3 inhibition on axons and dendrites of neurons grown with glia conditioning.

(G) Western blot analysis of the relative levels of different actin binding proteins in hippocampal neurons and Rat2 fibroblasts. Results are presented as a ratio of the level of the protein in the neurons relative to the level in the fibroblasts, such that a value greater than 1 indicates relatively more protein in neurons.

(H–J) N-WASP localization (red) in primary hippocampal neurons at different stages of development. N-WASP levels are relatively low in growth cones of undifferentiated neurites (H) and in growth cones of short axons (I). In longer axons, N-WASP becomes increasingly enriched in the distal axon and growth cone (J, arrow).

it is required for filopodia formation in neurons. Analysis of fixed neurons revealed that neurons expressing EGFP-CA had at least as many filopodia as control neurons expressing EGFP or EGFP-C (Figure 8A; the slight increase in EGFP-CA compared to controls was not statistically significant). Surprisingly, neurons expressing VCA had significantly more filopodia than both controls and EGFP-CA-expressing neurons. Whether this reflects a function of the V region or an increase in the efficacy of VCA as compared to CA remains to be determined.

To test the requirement for the Arp2/3 complex in de novo filopodia formation in response to a guidance cue, we examined the response of neurons to the guidance molecule Netrin-1, which is an attractive signal to these neurons. Bath application of Netrin-1 to cultured pyramidal neurons elicits a significant increase in the number of filopodia within 40 min of application (Dent et al., 2004; Lebrand et al., 2004). Application of 600 ng/ml recombinant mouse Netrin1 to hippocampal neurons expressing EGFP or EGFP-C lead to an increase in the number of filopodia after 40 min (Figures 8B–8D). This response was not inhibited by expression of EGFP-CA or VCA, indicating that Arp2/3 is not required for de novo filopodia formation under these circumstances.

Discussion

Arp2/3 Is a Negative Regulator Role of Growth Cone Translocation

In cell types where Arp2/3 plays an essential role in generating the actin-based protrusive force that drives motility, its function appears to be tightly coupled to its localization at the periphery (Bailly et al., 1999, 2001;

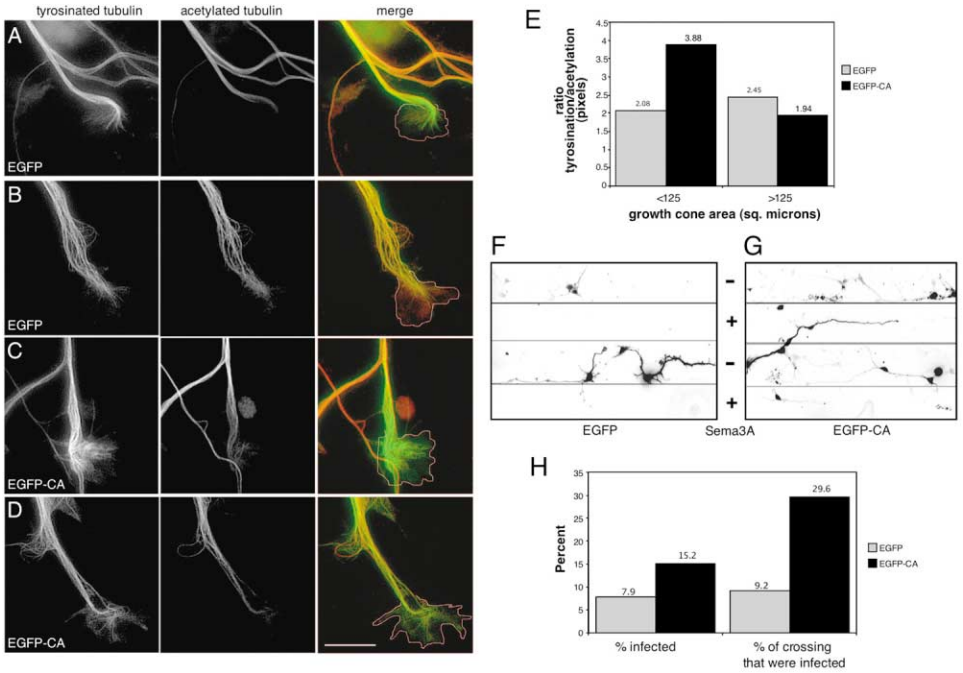

Figure 7. Arp2/3 Plays a Role in Regulating Growth Cone Microtubule Dynamics and Guidance

(A–D) Representative images of growth cones expressing control EGFP (A and B) or EGFP-CA (C and D) that were double labeled with antibodies to tyrosinated tubulin and acetylated tubulin. In the merged images, tyrosinated tubulin is green, acetylated tubulin is red, and overlap appears yellow. The dashed lines trace the growth cone perimeter. Scale bar equals 10 μm.

(E) The pixel intensity within the growth cone is presented as a ratio of the intensity in the tyrosinated channel to that in the acetylated channel. There is a significant difference in tubulin tyrosination between small growth cones (<125 μm^2) treated with EGFP and EGFP-CA ($p < 0.03$) and between small and large growth cones treated with EGFP-CA ($p < 0.007$).

(F and G) Embryonic hippocampal neurons expressing EGFP (F) or EGFP-CA (G) were grown on coverslips coated with alternating stripes of poly-l-lysine plus Semaphorin 3A (Sema3A, inhibitory stripe [+]) and poly-l-lysine alone (permissive stripe [−]). Images are inverted so the signal (i.e., EGFP or EGFP-CA) appears dark. Cultures were also stained with anti-tubulin β III to visualize all the neurons (data not shown). Positioning of the stripes was visualized as described (see Experimental Procedures) and is indicated by plus and minus signs between (F) and (G).

(H) Quantitation of the effect of EGFP-CA on neuron growth on/across inhibitory stripes.

Machesky and Insall, 1998; Svitkina and Borisy, 1999; Welch et al., 1997b). It was widely assumed that Arp2/3 would play a similar role in the growth cone periphery; however, we found that Arp2/3 is enriched in the central region of the growth cone and that there is relatively little Arp2/3 at the growth cone periphery. Similar results were obtained in hippocampal and DRG neurons using multiple different antisera to Arp2/3 and using p21-EGFP-tagged Arp2/3, suggesting that Arp2/3 function is likely to be most important in the central region of the growth cone.

Although it is possible that Arp2/3 acts at very low levels to generate a dendritic actin array at the growth cone periphery, EM analysis revealed relatively few branched filaments in the growth cone periphery (Figure 2). Instead, this region appears to be dominated by long actin filaments that are roughly perpendicular to the distal edge of the growth cone. Similar actin organization was seen in growth cones of all shapes and sizes and in both convex and concave areas of the growth cone, which are typically associated with membrane protrusion and retraction, respectively (Figure 2). These data are in agreement with previous studies (Letourneau, 1983; Lewis and Bridgman, 1992; Schaefer et al., 2002) that used several different EM protocols to visualize the growth cone cytoskeleton and observed that the peripheral region is primarily composed of two populations of actin filaments: long filaments oriented parallel to the membrane and shorter, randomly oriented filaments. Neither group detected a dendritic array of short Y-branched filaments indicative of Arp2/3 activity.

If Arp2/3 is not a major determinant of actin organization in the growth cone periphery, then functional inhibition should have little effect on the actin organization in this region. Indeed, growth cones expressing the Arp2/3 inhibitor (EGFP-CA) were indistinguishable from controls by immunofluorescence (Figures 5A–5F). At the EM level, there was no detectable change in actin filament organization (Figures 5G–5I), but there was sometimes a reduction in filament density (Figure 5I). These results contrast sharply with the dramatic changes in actin filament organization seen in Rat2 fibroblasts expressing EGFP-CA (Figure 4). Similar results were obtained with a construct containing the VCA domains of Wave-1 (data not shown). Although the high number of glia makes it difficult to do experiments with adenoviruses in DRG cultures, the similar localization of Arp2/3 in the central region of hippocampal and DRG growth cones suggests that Arp2/3 has a similar function in both populations of neurons.

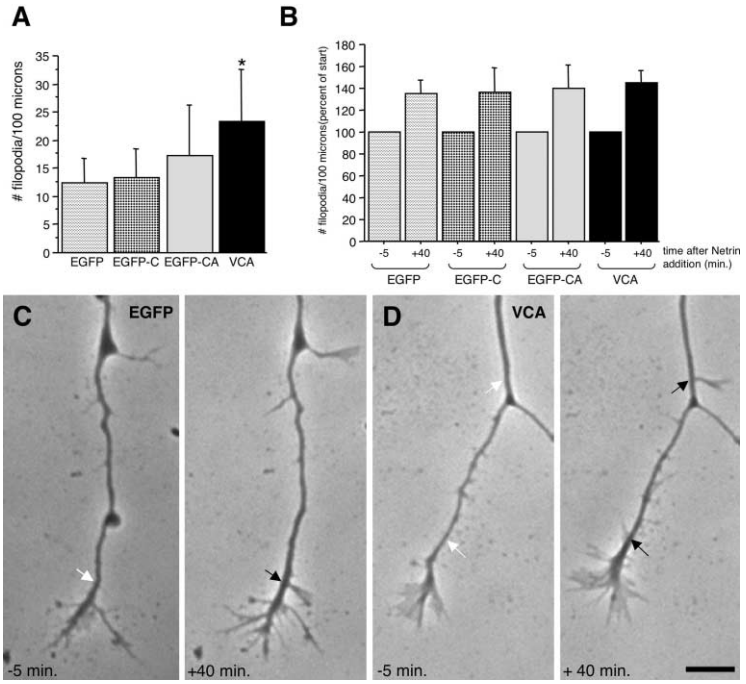

Figure 8. Arp2/3 Is not Required for Filopodia Formation

The requirement for Arp2/3 for filopodia formation was examined in both fixed (A) and living (B–D) neurons.

(A) Analysis of filopodia number in fixed cells. Neurons were infected with viruses 12–24 hr after plating. Approximately 48 hr after plating, neurons were fixed and stained with anti-tubulin β III and phalloidin. Infected cells were identified by EGFP expression and the number of filopodia counted. There was no significant difference between EGFP and EGFP-C. There was a slight, but not statistically significant, increase in the number of filopodia in EGFP-CA-expressing neurons relative to the EGFP and EGFP-C controls. VCA-expressing neurons showed a very significant ($p \leq 0.0001$) increase in filopodia number relative to EGFP and EGFP-C and significant increase ($p \leq 0.034$) relative to EGFP-CA.

(B) Analysis of filopodia induction in living neurons. Neurons were infected with viruses 12–24 hr after plating. Approximately 36 hr after plating, dishes were transferred to the microscope incubator and imaged at 25 s intervals for 10 min to determine that the growth cone was dynamically changing. Netrin1 (600 ng/ml) was then added directly to the bath and imaging was continued for an additional 60 min. Data represent the average number of filopodia over the 5 min proceeding Netrin1 addition ($T = -5$) or from 40 to 45 min after Netrin1 addition ($T = +40$). Error bars indicate ±1 standard deviation.

(C and D) Representative images of neurons expressing EGFP (C) or VCA (D) 5 min before (−5 min) or 40 min after (+40 min) addition of Netrin1. Black arrows indicate filopodia that formed de novo in regions where there were no filopodia at −5 min (white arrows). Scale bar equals 10 μm.

In fibroblasts, inhibition of Arp2/3 activity alters membrane protrusion (Bailly et al., 2001), indicating that Arp2/3-dependent actin filament branching activity plays an essential role in generating the force that drives membrane protrusion. Our results indicate that in growth cones, Arp2/3 is not essential for membrane protrusion, but it does play a critical role in regulating elongation in actively translocating axon growth cones. In *Drosophila,* null mutants in Arp2/3 and the Scar exhibit defects in many tissues, including the nervous system (Zallen et al., 2002). Flies with neuron-specific deletion of Arp2/3 or Scar elaborate apparently normal axons, further supporting our conclusion that Arp2/3 is not required for axon outgrowth per se (J. Ng and L. Luo, personal communication).

Mechanism of Arp2/3 Function in Growth Cones

Recent studies have shown that there is a direct correlation between the levels of tyrosinated microtubules and the rate of axon elongation (Bamburg, 2003; Rochlin et al., 1996). Other studies have implicated actin structures in the regulation of microtubule dynamics, which in turn affects growth cone motility, pausing, pathfinding, and axon branching (Dent et al., 1999; Dent and Kalil, 2001; Rodriguez et al., 2003; Zhou et al., 2002). In this context, our finding that inhibition of Arp2/3 activity in neurons alters the relative levels of tyrosinated microtubules and results in pathfinding defects suggests that Arp2/3-dependent actin structures normally function to regulate growth cone microtubules. This activity is particularly important during growth cone turning. Inhibition of Arp2/3 removes this regulation, which enhances microtubule dynamics and in turn enhances neurite elongation. This inappropriate tendency toward elongation may indirectly render the growth cone unable to obey a repulsive cue in a timely manner.

Although the density of actin and microtubules in the central region of the growth cone makes visualization of this region difficult (Figure 2), it is likely that Arp2/3 nucleates the formation of Y branches in growth cones, just as in fibroblasts. These Arp2/3-dependent actin structures may regulate microtubule dynamics either by serving as a type of barrier or "net" that retards microtubule advance, or by physical association with microtubules. One study in particular found a specific role for the growth cone actin "meshwork" (the F-actin not incorporated into the actin bundles) in retarding dynamic microtubule advance into the peripheral region (Zhou et al., 2002), suggesting that Arp2/3-dependent actin structures may act as a barrier to microtubule advance. If the effect on microtubule dynamics involves physical interaction, it is likely that other protein(s) link the actin and microtubules, though it is formally possible that there are proteins that link Arp2/3 directly to microtubules.

The fact that Arp2/3 inhibition does not block filopodia induction suggests that neurons are able to generate the immediate filopodia response to guidance cues independently of Arp2/3. Whether Arp2/3 function is required for later steps in growth cone turning toward Netrin remains to be determined. Given that it is an integral part of the cytoskeleton, we predict that inhibi-

tion of Arp2/3 would alter growth cone turning and elongation in response to both attractive and repulsive signals.

Determinants of Growth Cone Morphology and Motility

Our results indicate that inhibition of Arp2/3 affects growth cone translocation and pathfinding without significantly altering overall growth cone morphology. The dendritic array and convergent-elongation models of lamellipodia and filopodia formation imply that whether cells form a lamellipodium dominated by a dendritic array (as in the fibroblast) or a structure dominated by filopodia (like a growth cone) will depend on the relative concentrations and types of actin binding activities present; the most abundant actin binding proteins will determine the overall morphology of the motile structure, while less abundant proteins may have modulatory roles.

Comparative Western blot analysis (Figure 6G) and immunolocalization studies (Cohan et al., 2001; Lanier et al., 1999) have shown that compared to fibroblasts, growth cones have relatively high levels of fascin bundling and Ena/VASP anticapping activities, which would be predicted to favor filopodia formation. We propose that abundant proteins such as fascin and Ena/VASP are the major determinants of growth cone morphology and membrane protrusion, while the less abundant Arp2/3 complex plays an important role in coordinating actin structures that can regulate microtubule dynamics and growth cone translocation. Such a model is supported by the observations that altering fascin bundling or Ena/VASP anticapping activity dramatically alters growth cone morphology and actin organization. Treatments that decrease fascin bundling activity lead to a rapid loss of actin bundles in growth cone filopodia (Cohan et al., 2001). Functional inhibition of Ena/VASP proteins inhibits filopodia formation and increases the density of disorganized actin filaments in the growth cone periphery, while increasing Ena/VASP activity leads to an increase in the number and length of growth cone filopodia and actin bundles (Lebrand et al., 2004).

Our experiments clearly demonstrate that Arp2/3 is not required for lamellipodia protrusion or de novo filopodia formation in neurons. In these experiments, however, Arp2/3 was inhibited after neurites were formed, so it remains possible that Arp2/3 is required for neurite initiation. While there is clearly a need for actin-nucleating activity in the motile growth cone, it may be fulfilled by other nucleating proteins such as the formins, which have been implicated in the formation of unbranched actin filaments in vitro and in keratinocytes (Kobielak, 2003). These findings reveal a surprising new role for Arp2/3 in growth cone translocation and guidance and provide further evidence for the importance of crosstalk between the actin and microtubule cytoskeletons in this process.

Experimental Procedures

Cell Culture

All media and supplements were purchased from GIBCO-BRL. Poly-D-lysine and fibronectin were purchased from Sigma. Hippocampal and glial cultures were produced from E16 and P0 mice, respectively, as previously described (Lanier et al., 1999). Except for the stripe assays, approximately 2×10^4 cells were plated on each 12 mm coverslip. After 4 hr, the media was replaced with either neuronal growth medium (MEM with Earle's salts, B27 supplement, 10 mM HEPES, and 0.6% D-glucose) that had been conditioned on glia for 48 hr immediately prior to use or with unconditioned Neurobasal media with B27 supplement, 0.5 mM glutamine, and 25 μM glutamate. Rat2 cells were grown in DME/5% fetal calf serum.

Adenovirus Construction and Infection

Replication-deficient recombinant adenoviruses were produced using the AdEasy system (He et al., 1998). EGFP, EGFP-C (residues 450–486 of bovine N-WASP), EGFP-CA (residues 468–505 of bovine N-WASP), and p21-EGFP were cloned by PCR and inserted into pShuttle CMV. The myc-tagged VCA (residues 444–559 of human Wave-1) was cloned by PCR and inserted into pAdTrack-CMV. The resulting plasmid expresses VCA under a CMV promoter, with a second CMV promoter expressing the EGFP marker. Virus was purified on a CsCl gradient and titered on 293HEK cells. Cells were infected with a multiplicity of infection (m.o.i.) of 25–50 infectious viruses per cell.

Listeria Infection

Listeria monocytogenes strain 10435 was a gift from Darren Higgins. *Listeria* cultures were grown at 30°C in brain heart infusion broth (BHI, Difco). Overnight cultures were centrifuged, rinsed once in PBS, and resuspended in a 1/10th volume of PBS and applied to Rat2 cultures. After 1 hr at 37°C for, Rat2 cultures were rinsed twice with the appropriate media and given fresh media supplemented with 10 μg/ml gentamicin. After 4 hr, cultures were fixed and processed for immunofluorescence. For studies on the effect of EGFP or EGP-CA expression, cells were infected with adenovirus 24 hr prior to infection with *Listeria*. Because CNS neurons are extremely refractive to *Listeria* infection (Dramsi et al., 1998), we were unable to use EGFP-CA to inhibit *Listeria* motility in hippocampal neurons.

Immunofluorescence

The following antisera were used: rabbit anti-p21-Arc, p34-Arc, and Arp3 (a gift from Matthew Welch); affinity purified rabbit anti-p34-Arc (a gift from Laura Machesky); mouse anti-Tubulin β III (Promega); rat anti-tyrosinated tubulin MAB1864 (Chemicon); mouse anti-acetylated tubulin clone 6-11B-1 (Sigma); C4 anti-actin (Boehringer Mannheim); rabbit anti-N-WASP antisera (gifts from M. Kirschner and T. Takenawa); and rabbit anti-Listeria O (Difco). Secondary antisera were from Jackson ImmunoResearch and phalloidins were from Molecular Probes. Fixation and permeabilization conditions were optimized for each antiserum but were identical for Rat2 cells and neurons labeled with a given set of antisera. Cells were fixed for 30 min at 37°C in PPS (4% paraformaldehyde in PHEM buffer [60 mM PIPES (pH 7.0), 25 mM HEPES (pH 7.0), 10 mM EGDT, 2 mM $MgCl_2$] with 0.12 M sucrose). After rinsing in PBS, coverslips were incubated in 10% fatty acid free bovine serum albumin (BSA) in PBS for 30 min, permeabilized for 10 min in 0.2% triton/PBS, rinsed, and reblocked in 10% BSA/PBS for 30 min. For anti-p21 and anti-p34 antisera provided by M. Welch, cells were fixed with PPS as described above, denatured with cold methanol for 3 min, then permeabilized and blocked as described above. In neurons, similar results were obtained with and without methanol, so the methanol step was omitted in order to allow phalloidin staining. For double labeling with anti-tyrosinated and anti-acetylated tubulin, cultures were simultaneously fixed and permeabilized in PPS supplemented with 0.25% glutaraldehyde, 10 μM Taxol, 1.3 μM phalloidin, and 0.1% triton. This mixture stabilizes microtubules and actin filaments, while extracting soluble tubulin dimers and actin monomers (Dent and Kalil, 2001). Incubations with primary and secondary antisera were done in the presence of 1% BSA/PBS, and coverslips were mounted with 2.5% 1,4-Diazabicyclo-[2.2.2]Octane/150 mM Tris (pH 8.0)/30% glycerol to reduce photo bleaching. Images were captured on a Nikon TE200 using DeltaVision software (API).

Platinum Replica Electron Microscopy

Correlative platinum replica electron microscopy was performed essentially as described (Svitkina and Borisy, 1998) with a few minor

modifications. Briefly, dissociated embryonic hippocampal neurons were cultured as described above on coverslips coated with a gold locator grid. EGFP-positive cells were located by live cell fluorescence microscopy, then immediately extracted for 4.5 min with 1% Triton X-100 in PEM buffer (100 mM PIPES [pH 6.8], 1 mM EGTA, 1 mM $MgCl_2$) containing 10 μM phalloidin, 10 μM Taxol, 0.2% gluteraldehyde, and 4.2% sucrose as an osmotic buffer. Coverslips were washed with PEM containing 1 μM phalloidin, 1 μM Taxol, and 1% sucrose, fixed in 0.1 M Na-cacodylate buffer (pH 7.3), 2% gluteraldehyde, and 1% sucrose and processed for electron microscopy. Cells previously identified as EGFP positive were relocated using the gold grid.

Measurement of Axon and Dendrite Length

Cultures were fixed with PPS as described above and stained with mouse anti-Tubulin β III (Promega) and Alexa 594 phalloidin (Molecular Probes). Infected cells were identified by EGFP expression, and images were taken using either a 20× (for axon and dendrite length measurements) or 40× (for filopodia measurements) plan-neofluar objective and Openlab software (Improvision). Images were saved as tiff files and assigned coded names, and neurites were manually traced using NIH Image 1.62 and the Neurite Labeling Macro v1.1 (available at ftp://rsbweb.nih.gov/pub/nih-image/user-macros/). For axon and dendrite length measurements, data represent the average of at least 50 different neurons from at least two different experiments. For filopodia counts in fixed cells, filopodia were identified by phalloidin staining and data represent the average of at least 25 neurons from two different experiments. Data were analyzed using Statview and significance was determined by ANOVA with Sheffe's post hoc analysis.

Live Cell Imaging and Filopodia Analysis

Rat2 cell were plated directly on fibronectin-coated Bioptechs dishes, while neuronal cultures were plated on 35 mm tissue culture dishes fitted with German glass coverslips ("special dishes;" Goslin and Banker, 1998) and coated with 1 mg/ml poly-D-lysine. Rat2 cells were grown in a low-bicarbonate medium as previously described (Bear et al., 2000). Neuronal cultures were plated as described above. For filopodia analysis, special dishes were transferred to a microscope humidified stage incubator that maintained the cultures at 5% CO_2. Time-lapse movies were made at 25 s intervals for 70 min. Filopodia on growth cones and on the distalmost 100 microns of the axon shaft were counted in successive images. Data represent the average over a 5 min interval from 2–4 movies and at least 2 different experiments and significance was determined by ANOVA and Sheffe's post hoc analysis. For filopodia induction by Netrin 1, the number of filopodia was normalized to the starting value.

Stripe Assay

Stripe matrices were produced using a silicon matrix as described (Vielmetter et al., 1990). Alkaline-phosphatase tagged Semaphorin 3A (Sema 3A) was expressed in HEK293 cells and harvested from the tissue culture media as previously described (Kobayashi et al., 1997) For stripe assays, 18 mm coverslips were coated with 1 mg/ml poly-D-lysine, rinsed, and air dried. The coverslip was then inverted onto the stripe maker and a mixture of Sema 3A and rabbit IgG perfused though the matrix, forming alternating 90 micron wide stripes of poly-lysine alone and poly-lysine with Sema3A (and rabbit IgG). As a control, BSA was substituted for Sema 3A at the same concentration. Approximately 5×10^5 neurons were plated on each coverslip. After fixation, the Sema3A stripes were identified by labeling with a fluorescent anti-rabbit secondary.

Western Blot Analysis

To prepare extracts, cells were rinsed with PBS, lysed in extraction buffer (10 mM Tris [pH 8.0], 1% NP40, 150 mM NaCl supplemented with a protease inhibitor cocktail; Boehringer Mannheim), and centrifuged 10 min at 10,000 × g. Concentration of the extract was determined using the BCA protein assay (Pierce). SDS-PAGE and Western blot analysis were performed using standard techniques. In addition to the antisera used for immunofluorescence, the following antisera were used: mouse anti-cortactin mAb 4F11 (Upstate); mouse anti-capping protein β2 subunit mAb3F2.3 (Iowa Developmental Studies Hybridoma studies bank); rabbit anti-gelsolin (a gift from W. Witke), rabbit anti-cofilin (Cytoskeleton); mouse anti-α-actinin mAb BM-75.2 (Sigma); mouse anti-fascin mAb3582 (Chemicon International); monoclonal anti-zyxin (a gift from J. Wehland); rabbit anti-zyxin and mouse anti-paxilin (a gift from K. Burridge); mouse anti-vinculin and anti-paxillin (a gift from R. Salgia); rabbit anti-vinculin (a gift from K. Burridge); mouse anti-vinculin hVinc1 (Sigma); and rabbit anti-Mena, EVL, and VASP (produced in the Gertler lab). Secondary antibodies were from Jackson Labs. Signal was detected using the ECL reagent (Amersham-Pharmacia). Relative concentrations were determined using the NIH Image Gel Scanning macro. Each antiserum was tested at least twice on two different batches of extract and results are presented as an average ratio.

Acknowledgments

We are grateful to Drs. Matt Welch, Tadaomi Takenawa, Keith Burridge, Jurgen Wehland, Ravi Salgia, and Mark Kirschner for their generous gifts of antibodies, to Dr. Laura Machesky for the gift of antibodies and DNA constructs, and to Dr. Burt Vogelstein for the gift of AdEasy cloning vectors. We thank Drs. Julian Ng and Liqun Luo for sharing unpublished data. This work was supported by NIH grant #6895154 and a W.M. Keck Distinguished Young Scholar Award to F.B.G. and Minnesota Medical Foundation grant #333-9238-03 and Academic Health Center Seed grant #2003-39 to L.M.L.

Received: September 12, 2003
Revised: March 10, 2004
Accepted: May 18, 2004
Published: July 7, 2004

References

Amann, K.J., and Pollard, T.D. (2001). The Arp2/3 complex nucleates actin filament branches from the sides of pre-existing filaments. Nat. Cell Biol. *3*, 306–310.

Arce, C.A., Hallak, M.E., Rodriguez, J.A., Barra, H.S., and Caputto, R. (1978). Capability of tubulin and microtubules to incorporate and to release tyrosine and phenylalanine and the effect of the incorporation of these amino acids on tubulin assembly. J. Neurochem. *31*, 205–210.

Bailly, M., Macaluso, F., Cammer, M., Chan, A., Segall, J.E., and Condeelis, J.S. (1999). Relationship between Arp2/3 complex and the barbed ends of actin filaments at the leading edge of carcinoma cells after epidermal growth factor stimulation. J. Cell Biol. *145*, 331–345.

Bailly, M., Ichetovkin, I., Grant, W., Zebda, N., Machesky, L.M., Segall, J.E., and Condeelis, J. (2001). The F-actin side binding activity of the Arp2/3 complex is essential for actin nucleation and lamellipod extension. Curr. Biol. *11*, 620–625.

Bamburg, J.R. (2003). Introduction to cytoskeletal dynamics and pathfinding of neuronal growth cones. J. Histochem. Cytochem. *51*, 407–409.

Bamburg, J.R., Bray, D., and Chapman, K. (1986). Assembly of microtubules at the tip of growing axons. Nature *321*, 788–790.

Banzai, Y., Miki, H., Yamaguchi, H., and Takenawa, T. (2000). Essential role of neural Wiskott-Aldrich syndrome protein in neurite extension in PC12 cells and rat hippocampal primary culture cells. J. Biol. Chem. *275*, 11987–11992.

Bear, J.E., Loureiro, J.J., Libova, I., Fassler, R., Wehland, J., and Gertler, F.B. (2000). Negative regulation of fibroblast motility by Ena/VASP proteins. Cell *101*, 717–728.

Bear, J.E., Svitkina, T.M., Krause, M., Schafer, D.A., Loureiro, J.J., Strasser, G.A., Maly, I.V., Chaga, O.Y., Cooper, J.A., Borisy, G.G., and Gertler, F.B. (2002). Antagonism between Ena/VASP proteins and actin filament capping regulates fibroblast motility. Cell *109*, 509–521.

Bentley, D., and Toroian-Raymond, A. (1986). Disoriented pathfinding by pioneer neurone growth cones deprived of filopodia by cytochalasin treatment. Nature *323*, 712–715.

Bretscher, A., Edwards, K., and Fehon, R.G. (2002). ERM proteins and merlin: integrators at the cell cortex. Nat. Rev. Mol. Cell Biol. *3*, 586–599.

Buck, K.B., and Zheng, J.Q. (2002). Growth cone turning induced by direct local modification of microtubule dynamics. J. Neurosci. *22*, 9358–9367.

Caldwell, J.E., Waddle, J.A., Cooper, J.A., Hollands, J.A., Casella, S.J., and Casella, J.F. (1989). cDNAs encoding the beta subunit of cap Z, the actin-capping protein of the Z line of muscle. J. Biol. Chem. *264*, 12648–12652.

Challacombe, J.F., Snow, D.M., and Letourneau, P.C. (1997). Dynamic microtubule ends are required for growth cone turning to avoid an inhibitory guidance cue. J. Neurosci. *17*, 3085–3095.

Chien, C.B., Rosenthal, D.E., Harris, W.A., and Holt, C.E. (1993). Navigational errors made by growth cones without filopodia in the embryonic *Xenopus* brain. Neuron *11*, 237–251.

Cohan, C., Welnhofer, E., Zhao, L., Matsumura, F., and Yamashiro, S. (2001). Role of the actin bundling protein fascin in growth cone morphogenesis: localization in filopodia and lamellipodia. Cell Motil. Cytoskeleton *48*, 109–120.

Cooper, J.A., and Schafer, D.A. (2000). Control of actin assembly and disassembly at filament ends. Curr. Opin. Cell Biol. *12*, 97–103.

Dent, E.W., and Kalil, K. (2001). Axon branching requires interactions between dynamic microtubules and actin filaments. J. Neurosci. *21*, 9757–9769.

Dent, E.W., Callaway, J.L., Szebenyi, G., Baas, P.W., and Kalil, K. (1999). Reorganization and movement of microtubules in axonal growth cones and developing interstitial branches. J. Neurosci. *19*, 8894–8908.

Dent, E.W., Barnes, A., Tang, F., and Kalil, K. (2004). Netrin-1 and Sema 3A promote or inhibit cortical axon branching respectively by reorganization of the cytoskeleton. J. Neurosci., in press.

Dickson, B.J. (2002). Molecular mechanisms of axon guidance. Science *298*, 1959–1964.

Dramsi, S., Levi, S., Triller, A., and Cossart, P. (1998). Entry of *Listeria monocytogenes* into neurons occurs by cell-to-cell spread: an in vitro study. Infect. Immun. *66*, 4461–4468.

Du, Y., Weed, S.A., Xiong, W.C., Marshall, T.D., and Parsons, J.T. (1998). Identification of a novel cortactin SH3 domain-binding protein and its localization to growth cones of cultured neurons. Mol. Cell. Biol. *18*, 5838–5851.

Falet, H., Hoffmeister, K.M., Neujahr, R., Italiano, J.E., Jr., Stossel, T.P., Southwick, F.S., and Hartwig, J.H. (2002). Importance of free actin filament barbed ends for Arp2/3 complex function in platelets and fibroblasts. Proc. Natl. Acad. Sci. USA *99*, 16782–16787.

Gomez, T.M., and Letourneau, P.C. (1994). Filopodia initiate choices made by sensory neuron growth cones at laminin/fibronectin borders in vitro. J. Neurosci. *14*, 5959–5972.

Goslin, K., and Banker, G. (1998). Rat hippocampal neurons in low density culture. In Culturing Nerve Cells, G. Banker and K. Goslin, eds. (Cambridge, MA: MIT Press), pp. 339–370.

Gungabissoon, R.A., and Bamburg, J.R. (2003). Regulation of growth cone actin dynamics by ADF/cofilin. J. Histochem. Cytochem. *51*, 411–420.

He, T.C., Zhou, S., da Costa, L.T., Yu, J., Kinzler, K.W., and Vogelstein, B. (1998). A simplified system for generating recombinant adenoviruses. Proc. Natl. Acad. Sci. USA *95*, 2509–2514.

Hufner, K., Higgs, H.N., Pollard, T.D., Jacobi, C., Aepfelbacher, M., and Linder, S. (2001). The verprolin-like central (vc) region of Wiskott-Aldrich syndrome protein induces Arp2/3 complex-dependent actin nucleation. J. Biol. Chem. *276*, 35761–35767.

Hufner, K., Schell, B., Aepfelbacher, M., and Linder, S. (2002). The acidic regions of WASp and N-WASP can synergize with CDC42Hs and Rac1 to induce filopodia and lamellipodia. FEBS Lett. *514*, 168–174.

Kim, G.J., Shatz, C.J., and McConnell, S.K. (1991). Morphology of pioneer and follower growth cones in the developing cerebral cortex. J. Neurobiol. *22*, 629–642.

Kim, M.D., Kolodziej, P., and Chiba, A. (2002). Growth cone pathfinding and filopodial dynamics are mediated separately by Cdc42 activation. J. Neurosci. *22*, 1794–1806.

Kobayashi, H., Koppel, A.M., Luo, Y., and Raper, J.A. (1997). A role for collapsin-1 in olfactory and cranial sensory axon guidance. J. Neurosci. *17*, 8339–8352.

Kobielak, A., Pasolli, H.A., and Fuchs, E. (2004). Mammalian formin-1 participates in adherens junctions and polymerization of linear actin cables. Nat. Cell Biol. *6*, 21–30.

Koleske, A.J. (2003). Do filopodia enable the growth cone to find its way? Sci STKE, pe20.

Kuhn, T.B., Williams, C.V., Dou, P., and Kater, S.B. (1998). Laminin directs growth cone navigation via two temporally and functionally distinct calcium signals. J. Neurosci. *18*, 184–194.

Kureishy, N., Sapountzi, V., Prag, S., Anilkumar, N., and Adams, J.C. (2002). Fascins, and their roles in cell structure and function. Bioessays *24*, 350–361.

L'Hernault, S.W., and Rosenbaum, J.L. (1985). Chlamydomonas alpha-tubulin is posttranslationally modified by acetylation on the epsilon-amino group of a lysine. Biochemistry *24*, 473–478.

Lanier, L.M., Gates, M.A., Witke, W., Menzies, A.S., Wehman, A.M., Macklis, J.D., Kwiatkowski, D., Soriano, P., and Gertler, F.B. (1999). Mena is required for neurulation and commissure formation. Neuron *22*, 313–325.

Lebrand, C., Dent, E.W., Strasser, G.A., Lanier, L.M., Krause, M., Svitkina, T.M., Borisy, G.G., and Gertler, F.B. (2004). Critical role of Ena/VASP proteins for filopodia formation in neurons and function downstream of Netrin-1. Neuron *42*, 37–49.

Le Gal La Salle, G., Robert, J.J., Berrard, S., Ridoux, V., Stratford-Perricaudet, L.D., Perricaudet, M., and Mallet, J. (1993). An adenovirus vector for gene transfer into neurons and glia in the brain. Science *259*, 988–990.

Letourneau, P.C. (1983). Differences in the organization of actin in the growth cones compared with the neurites of cultured neurons from chick embryos. J. Cell Biol. *97*, 963–973.

Lewis, A.K., and Bridgman, P.C. (1992). Nerve growth cone lamellipodia contain two populations of actin filaments that differ in organization and polarity. J. Cell Biol. *119*, 1219–1243.

Lin, C.H., and Forscher, P. (1993). Cytoskeletal remodeling during growth cone-target interactions. J. Cell Biol. *121*, 1369–1383.

Lu, M., Witke, W., Kwiatkowski, D.J., and Kosik, K.S. (1997). Delayed retraction of filopodia in gelsolin null mice. J. Cell Biol. *138*, 1279–1287.

Luo, L. (2002). Actin cytoskeleton regulation in neuronal morphogenesis and structural plasticity. Annu. Rev. Cell Dev. Biol. *18*, 601–635.

Machesky, L.M., and Insall, R.H. (1998). Scar1 and the related Wiskott-Aldrich syndrome protein, WASP, regulate the actin cytoskeleton through the Arp2/3 complex. Curr. Biol. *8*, 1347–1356.

Machesky, L.M., Reeves, E., Wientjes, F., Mattheyse, F.J., Grogan, A., Totty, N.F., Burlingame, A.L., Hsuan, J.J., and Segal, A.W. (1997). Mammalian actin-related protein 2/3 complex localizes to regions of lamellipodial protrusion and is composed of evolutionarily conserved proteins. Biochem. J. *328*, 105–112.

Machesky, L.M., Mullins, R.D., Higgs, H.N., Kaiser, D.A., Blanchoin, L., May, R.C., Hall, M.E., and Pollard, T.D. (1999). Scar, a WASp-related protein, activates nucleation of actin filaments by the Arp2/3 complex. Proc. Natl. Acad. Sci. USA *96*, 3739–3744.

Marchand, J.B., Kaiser, D.A., Pollard, T.D., and Higgs, H.N. (2001). Interaction of WASP/Scar proteins with actin and vertebrate Arp2/3 complex. Nat. Cell Biol. *3*, 76–82.

Marsh, L., and Letourneau, P.C. (1984). Growth of neurites without filopodial or lamellipodial activity in the presence of cytochalasin B. J. Cell Biol. *99*, 2041–2047.

Mason, C., and Erskine, L. (2000). Growth cone form, behavior, and interactions in vivo: retinal axon pathfinding as a model. J. Neurobiol. *44*, 260–270.

May, R.C., Hall, M.E., Higgs, H.N., Pollard, T.D., Chakraborty, T., Wehland, J., Machesky, L.M., and Sechi, A.S. (1999). The Arp2/3 complex is essential for the actin-based motility of *Listeria monocytogenes*. Curr. Biol. *9*, 759–762.

Meberg, P.J., and Bamburg, J.R. (2000). Increase in neurite outgrowth mediated by overexpression of actin depolymerizing factor. J. Neurosci. *20*, 2459–2469.

Miki, H., and Takenawa, T. (1998). Direct binding of the verprolin-homology domain in N-WASP to actin is essential for cytoskeletal reorganization. Biochem. Biophys. Res. Commun. *243*, 73–78.

Miki, H., Miura, K., and Takenawa, T. (1996). N-WASP, a novel actin-depolymerizing protein, regulates the cortical cytoskeletal rearrangement in a PIP2-dependent manner downstream of tyrosine kinases. EMBO J. *15*, 5326–5335.

Paglini, G., Kunda, P., Quiroga, S., Kosik, K., and Caceres, A. (1998). Suppression of radixin and moesin alters growth cone morphology, motility, and process formation In primary cultured neurons. J. Cell Biol. *143*, 443–455.

Pollard, T.D. (2002). Formins initiate new actin filaments. Nat. Cell Biol. *4*, E191.

Pollard, T.D., and Beltzner, C.C. (2002). Structure and function of the Arp2/3 complex. Curr. Opin. Struct. Biol. *12*, 768–774.

Pollard, T.D., and Borisy, G.G. (2003). Cellular motility driven by assembly and disassembly of actin filaments. Cell *113*, 549.

Rochlin, M.W., Wickline, K.M., and Bridgman, P.C. (1996). Microtubule stability decreases axon elongation but not axoplasm production. J. Neurosci. *16*, 3236–3246.

Rochlin, M.W., Dailey, M.E., and Bridgman, P.C. (1999). Polymerizing microtubules activate site-directed F-actin assembly in nerve growth cones. Mol. Biol. Cell *10*, 2309–2327.

Rodriguez, O.C., Schaefer, A.W., Mandato, C.A., Forscher, P., Bement, W.M., and Waterman-Storer, C.M. (2003). Conserved microtubule-actin interactions in cell movement and morphogenesis. Nat. Cell Biol. *5*, 599–609.

Rohatgi, R., Ma, L., Miki, H., Lopez, M., Kirchhausen, T., Takenawa, T., and Kirschner, M.W. (1999). The interaction between N-WASP and the Arp2/3 complex links Cdc42-dependent signals to actin assembly. Cell *97*, 221–231.

Schaefer, A.W., Kabir, N., and Forscher, P. (2002). Filopodia and actin arcs guide the assembly and transport of two populations of microtubules with unique dynamic parameters in neuronal growth cones. J. Cell Biol. *158*, 139–152.

Stossel, T.P., Condeelis, J., Cooley, L., Hartwig, J.H., Noegel, A., Schleicher, M., and Shapiro, S.S. (2001). Filamins as integrators of cell mechanics and signalling. Nat. Rev. Mol. Cell Biol. *2*, 138–145.

Suter, D.M., Errante, L.D., Belotserkovsky, V., and Forscher, P. (1998). The Ig superfamily cell adhesion molecule, apCAM, mediates growth cone steering by substrate-cytoskeletal coupling. J. Cell Biol. *141*, 227–240.

Svitkina, T.M., and Borisy, G.G. (1998). Correlative light and electron microscopy of the cytoskeleton of cultured cells. Methods Enzymol. *298*, 570–592.

Svitkina, T.M., and Borisy, G.G. (1999). Arp2/3 complex and actin depolymerizing factor/cofilin in dendritic organization and treadmilling of actin filament array in lamellipodia. J. Cell Biol. *145*, 1009–1026.

Svitkina, T.M., Verkhovsky, A.B., and Borisy, G.G. (1995). Improved procedures for electron microscopic visualization of the cytoskeleton of cultured cells. J. Struct. Biol. *115*, 290–303.

Svitkina, T.M., Bulanova, E.A., Chaga, O.Y., Vignjevic, D.M., Kojima, S., Vasiliev, J.M., and Borisy, G.G. (2003). Mechanism of filopodia initiation by reorganization of a dendritic network. J. Cell Biol. *160*, 409–421.

Symons, M., Derry, J.M., Karlak, B., Jiang, S., Lemahieu, V., McCormick, F., Francke, U., and Abo, A. (1996). Wiskott-Aldrich syndrome protein, a novel effector for the GTPase CDC42Hs, is implicated in actin polymerization. Cell *84*, 723–734.

Szebenyi, G., Dent, E.W., Callaway, J.L., Seys, C., Lueth, H., and Kalil, K. (2001). Fibroblast growth factor-2 promotes axon branching of cortical neurons by influencing morphology and behavior of the primary growth cone. J. Neurosci. *21*, 3932–3941.

Tanaka, E., Ho, T., and Kirschner, M.W. (1995). The role of microtubule dynamics in growth cone motility and axonal growth. J. Cell Biol. *128*, 139–155.

Tanaka, E., and Kirschner, M.W. (1995). The role of microtubules in growth cone turning at substrate boundaries. J. Cell Biol. *128*, 127–137.

Tessier-Lavigne, M., and Goodman, C.S. (1996). The molecular biology of axon guidance. Science *274*, 1123–1133.

Tosney, K.W., and Landmesser, L.T. (1985). Growth cone morphology and trajectory in the lumbosacral region of the chick embryo. J. Neurosci. *5*, 2345–2358.

Vielmetter, J., Stolze, B., Bonhoeffer, F., and Stuermer, C.A. (1990). In vitro assay to test differential substrate affinities of growing axons and migratory cells. Exp. Brain Res. *81*, 283–287.

Vignjevic, D., Yarar, D., Welch, M.D., Peloquin, J., Svitkina, T., and Borisy, G.G. (2003). Formation of filopodia-like bundles in vitro from a dendritic network. J. Cell Biol. *160*, 951–962.

Weaver, A.M., Karginov, A.V., Kinley, A.W., Weed, S.A., Li, Y., Parsons, J.T., and Cooper, J.A. (2001). Cortactin promotes and stabilizes Arp2/3-induced actin filament network formation. Curr. Biol. *11*, 370–374.

Weaver, A.M., Young, M.E., Lee, W.L., and Cooper, J.A. (2003). Integration of signals to the Arp2/3 complex. Curr. Opin. Cell Biol. *15*, 23–30.

Weed, S.A., Karginov, A.V., Schafer, D.A., Weaver, A.M., Kinley, A.W., Cooper, J.A., and Parsons, J.T. (2000). Cortactin localization to sites of actin assembly in lamellipodia requires interactions with F-actin and the Arp2/3 complex. J. Cell Biol. *151*, 29–40.

Welch, M.D., DePace, A.H., Verma, S., Iwamatsu, A., and Mitchison, T.J. (1997a). The human Arp2/3 complex is composed of evolutionarily conserved subunits and is localized to cellular regions of dynamic actin filament assembly. J. Cell Biol. *138*, 375–384.

Welch, M.D., Iwamatsu, A., and Mitchison, T.J. (1997b). Actin polymerization is induced by Arp2/3 protein complex at the surface of *Listeria monocytogenes*. Nature *385*, 265–269.

Wills, Z., Bateman, J., Korey, C.A., Comer, A., and Van Vactor, D. (1999). The tyrosine kinase Abl and its substrate enabled collaborate with the receptor phosphatase Dlar to control motor axon guidance. Neuron *22*, 301–312.

Winter, D., Lechler, T., and Li, R. (1999). Activation of the yeast Arp2/3 complex by Bee1p, a WASP-family protein. Curr. Biol. *9*, 501–504.

Yu, T.W., and Bargmann, C.I. (2001). Dynamic regulation of axon guidance. Nat. Neurosci. *4* (*Suppl*), 1169–1176.

Zalevsky, J., Lempert, L., Kranitz, H., and Mullins, R.D. (2001). Different WASP family proteins stimulate different Arp2/3 complex-dependent actin-nucleating activities. Curr. Biol. *11*, 1903–1913.

Zallen, J.A., Cohen, Y., Hudson, A.M., Cooley, L., Wieschaus, E., and Schejter, E.D. (2002). SCAR is a primary regulator of Arp2/3-dependent morphological events in *Drosophila*. J. Cell Biol. *156*, 689–701.

Zheng, J.Q., Wan, J.J., and Poo, M.M. (1996). Essential role of filopodia in chemotropic turning of nerve growth cone induced by a glutamate gradient. J. Neurosci. *16*, 1140–1149.

Zhou, F.Q., Waterman-Storer, C.M., and Cohan, C.S. (2002). Focal loss of actin bundles causes microtubule redistribution and growth cone turning. J. Cell Biol. *157*, 839–849.